Journal of Power Sources 187 (2009) 275–283

Contents lists available at ScienceDirect

Journal of Power Sources

journal homepage: www.elsevier.com/locate/jpowsour

Effect of Fe-contamination on rate of self-discharge in carbon-based aqueous electrochemical capacitors

Heather A. Andreas*, Kate Lussier, Alicia M. Oickle

Department of Chemistry, Dalhousie University, Halifax, NS, Canada B3H 4J3

ARTICLE INFO

Article history:
Received 8 September 2008
Received in revised form 22 October 2008
Accepted 22 October 2008
Available online 5 November 2008

Keywords:
Self-discharge
Iron contamination
Electrochemical capacitor
Carbon electrode
Aqueous electrolyte

ABSTRACT

The effect of Fe concentration on the Fe-induced self-discharge of electrochemical capacitor carbon electrodes in aqueous H_2SO_4 is presented. With an Fe-free system, the positive electrode self-discharges via an activation controlled self-discharge mechanism, while the negative electrode self-discharges with a diffusion control profile. This highlights that the self-discharge mechanism on each electrode of an electrochemical capacitor is likely different, and should be examined in a three-electrode (half cell) setup.

It is shown that Fe concentrations up to 10^{-5} M can be tolerated with no enhancement of self-discharge on the positive electrode. Whereas the negative carbon electrode can withstand Fe concentrations of 10^{-3} M without self-discharge increase. Additionally, it is shown that the diffusion controlled Fe-induced self-discharge (at concentrations at and above 10^{-4} M on the positive electrode) occurs primarily on the external surface of the porous electrode, and the carbon surface inside the pores does not participate in self-discharge. This is used to explain why the Conway diffusion model for self-discharge, derived for semi-infinite diffusion to a planar electrode, can be used to fit the self-discharge process on porous electrodes.

1. Introduction

Electrochemical capacitors (ECs), also called supercapacitors, ultracapacitors, and, in specific cases, double-layer capacitors, are energy-storage systems similar to batteries. In ECs, charge may be stored in redox reactions (similar to the charge storage in batteries), called pseudocapacitance, or charge may be stored in electrode-electrolyte double-layers [1]. Charge storage in the double-layer provides high power capabilities for double-layer capacitors and very high cycle life. However, there is significantly less energy-density in double-layer capacitors relative to pseudocapacitive ECs, batteries or fuel cells, since only approximately 0.18 electrons are stored per surface atom in the double-layer, whereas 1 or 2 electrons are stored per surface atom in pseudocapacitive ECs, batteries or fuel cells [1].

Similar to batteries, both types of ECs may undergo a process of self-discharge, where the EC loses voltage (charge) as it sits in a charged state for significant periods of time [1]. This loss of voltage may be a significant factor limiting EC usage in various commercial applications, including uninterruptible power supply backup and electric vehicle applications, where the EC may sit unused for days or weeks at a time. At present, there is very little literature on self-discharge mechanisms for carbon-based aqueous ECs. Though the self-discharge rate is often recorded for new configurations, there is no systematic study in the literature regarding the underlying causes of the loss of charge with time.

To aid in the identification of the self-discharge mechanism of an EC electrode, Conway et al. [2,3] proposed mathematical models which predict the self-discharge profile shape based on three possible ways in which self-discharge may occur. It should be noted that these models were developed for single-electrodes, rather than for full systems, as the self-discharge profile of each electrode in a full cell is expected to be different. The first proposed mechanism was based on an activation controlled, non-diffusion controlled, self-discharge based on the Faradaic reaction of some species which is abundant in the cell or is confined to the surface. This situation was predicted to present a self-discharge profile which will be linear when plotted potential as a function of log time (after some time, θ) [2,3]. The second possible mechanism is self-discharge due to the Faradaic reaction of a diffusion-controlled species (i.e. the reacting species is at a low enough concentration that diffusion is the rate-limiting step). This situation resulted in a self-discharge profile which was linear when potential is plotted as a function of $t^{1/2}$ [2,3]. The third mechanism proposed by the Conway group was the ohmic leakage between the two electrodes resulting in a self-discharge profile that is linear as $\log V_t$ versus time [2,3].

Two possible self-discharge mechanisms are explored in the scientific literature. Electrolyte decomposition-induced self-

* Corresponding author. Tel.: +1 902 4944505; fax: +1 902 4941310.
E-mail address: heather.andreas@dal.ca (H.A. Andreas).

0378-7753/$ – see front matter © 2008 Elsevier B.V. All rights reserved.
doi:10.1016/j.jpowsour.2008.10.096

discharge was mathematically modeled by Pillay and Newman [4], where they showed that the low concentrations of dissolved O_2 and H_2 in the ECs can shift the Nernstian potentials for water decomposition such that electrolyte decomposition may occur on the charged electrode surface, causing self-discharge when the charged system is placed on open-circuit. The scientific literature and the EC industry suggest that the carbons and electrolytes used in ECs may be contaminated with Fe, causing self-discharge due to an iron shuttle redox reaction, wherein Fe is oxidized on one electrode (discharging the positive electrode) and diffusing to the other electrode where it is reduced (discharging the negative electrode). Kazaryan et al. [5] examined this mechanism on the negative electrode of an asymmetric EC (the positive electrode is a PbO_2 battery-type electrode), and showed that Fe can enhance self-discharge at relatively high Fe concentrations (10^{-2} to 10^{-1} M) and that Fe has a much greater effect on self-discharge rate than other common metal impurities, such as W or Mn [6].

The effect of Fe-contaminant concentration on the self-discharge rate is presented here in order to determine the maximum Fe-contamination which does not result in an increased self-discharge rate for a symmetric carbon-based aqueous EC. Thus, the Fe-induced self-discharge of the positive carbon EC electrode was studied for the first time. Since the self-discharge profile of the positive and negative electrodes are likely different, a three-electrode (half cell) experimental setup is used to separate the effect of Fe on each electrode, highlighting where Fe has the greatest effect.

Finally, the research presented here was for relatively short self-discharge times (ca. 16 h). Kazaryan et al. [5] noted a significantly different self-discharge profile at these short times compared with the profiles at longer times, and attributed this to the effect of pores on the charging of the electrode. The pore effect is due to the solution resistance in the electrode pores causing the surface at the tip of the pore to charge more quickly than the surfaces deep in the pore [7,8]. Thus, after charging, there may be a distributed potential down the pores. When the system is placed on open-circuit the excess charges at the tip of the pore migrate deeper into the pore, and the potential of the electrode (which is measured at the pore tip) falls rapidly and the electrode appears to undergo a very rapid initial self-discharge process. In this work, the pore effect was reduced significantly to study the self-discharge profile at short self-discharge times with limited influence from the pore. A closer examination of this pore effect on the self-discharge profile is underway in the authors' laboratory.

2. Experimental

2.1. Electrode preparation and electrochemical cell

The carbon examined was Spectracarb 2225, a 2500 $m^2\,g^{-1}$ BET surface area woven carbon cloth material. This carbon was used as it has very little Fe-contamination, and Inductively Coupled Plasma - Mass Spectrometry experiments showed less than 10 ppm of Fe in this carbon. This allows for the precise control of the Fe-concentration, making it ideal for this work as it was then possible to contaminate the cell with known Fe concentrations, without residual carbon Fe-contaminants changing this concentration (other types of carbon may have significantly higher amounts Fe-contaminants than the carbon used here). Additionally, this carbon was chosen for its high surface area, as well as its ease of use since it does not require a binder, as would a carbon powder. The working electrode carbon (ca. 10 mg) is held in a specially made electrode holder composed of a Swagelok tube fitting sealed to a glass tube. An ionically insulating, electronically conducting Parafin-plasticized carbon (provided by Axion Power International, Inc.) is used as the current collector and electrical connection is made via a Pt wire.

The electrochemical measurements were performed in a three-electrode, three-compartment glass cell containing 100 mL of 1.0 M H_2SO_4 made from ultrapure H_2SO_4 (Aldrich, 99.999% purity) and 18 MΩ water. The counter electrode was a large piece of Spectracarb 2225 carbon cloth material wrapped with a gold wire for electrical connection. The reference electrode was a standard hydrogen electrode (SHE), and all potentials in this paper are referenced to it. The cell was deaerated before and during electrochemical experiments by bubbling N_2 through the working and counter electrode compartments. This research was all carried out at 22 ± 3 °C. A PAR VMP3/Z Multipotentiostat was used under EC-lab software control for data collection.

2.2. Electrochemical measurements

Prior to all self-discharge and Fe-contamination experiments, cyclic voltammetry was performed on the carbon electrodes between potential limits of 0.0 and 1.0 V versus SHE, using a sweep rate of 1 mV s^{-1}. The potential of the carbon electrodes was cycled until the cyclic voltammogram (CV) reached steady-state (typically 300–400 cycles, depending on the electrode), at which point there was no longer any change to the shape or size of the CV. This step was required before self-discharge measurements since each carbon evidenced quinone group development during this initial cycling step (see Section 3.1).

Self-discharge measurements were performed on multiple (at least five) carbon electrodes by charging each electrode from 0.5 V to the desired potential (0.0 or 1.0 V) using a potential ramp rate of 1 mV s^{-1}. The initial potential of 0.5 V was chosen as this was close to the average open-circuit potential (OCP) of the Spectracarb 2225 electrodes (although there was some variation in the OCP between electrodes). This potential was taken as the "uncharged" state of the electrode. The upper potential of 1.0 V was used since, with this carbon, the application of higher potentials causes irreversible damage to the electrode, reducing its capacitance and increasing electrode resistance. The negative potential of 0.0 V was chosen because below this potential another undesired, irreversible redox reaction occurs. A holding step at the desired charged potential was then introduced of duration between 0 s and 10 h. The cell was then placed on open-circuit and the potential was measured as a function of time for up to 16 h of self-discharge. During the self-discharge measurement, data points are recorded every ms for the first 1 s, followed by every 0.1 s for 2 min and then every 20 s for 2 h, and finally, every 120 s for 14 h. This number of points was chosen as it provides a sufficient number of points without changing the self-discharge curve due to oversampling.

2.3. Fe-contamination experiments

While the carbon and electrolyte used in this work were free of Fe-contaminants, the contamination that may be expected in "real" EC systems may be much higher. To test the effect of various degrees of Fe-contamination, the cell was artificially contaminated with Fe. The Fe "contaminant" was added to the electrochemical cell to provide concentrations ranging from 10^{-8} to 10^{-1} M. The iron was added as both ferrous sulfate ($FeSO_4{\cdot}7H_2O$, Fisher Scientific, ACS grade) and ferric sulfate ($Fe_2(SO_4)_3{\cdot}xH_2O$, Mallinckrodt Baker, AR grade). An approximately equimolar concentration of ferric and ferrous sulfate was used in the electrochemical cell to ensure that the Nernstian potential for $Fe^{3+} + 1e^- \rightarrow Fe^{2+}$ did not shift from its standard reduction potential of 0.77 V [9], as a shift of this potential between experiments may spuriously affect the self-discharge rate.

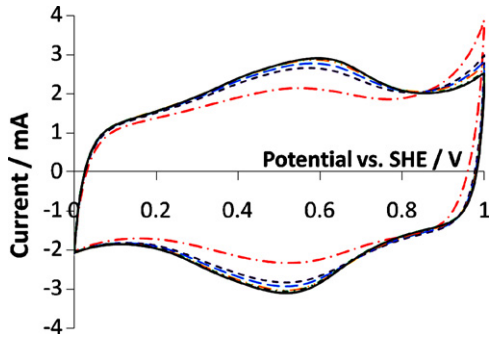

Fig. 1. Cyclic voltammogram of Spectracarb 2225 carbon-cloth (ca. 10 mg) in 1.0 M H_2SO_4 using a sweep rate of 1 mV s^{-1}, showing the cycling to steady-state and quinone peak development at ca. 0.5 V, cycle 3 ( ); cycle 50 ( ); cycle 100 ( ), cycle 200 ( ), cycle 300 ( ) and cycle 425 ( ).

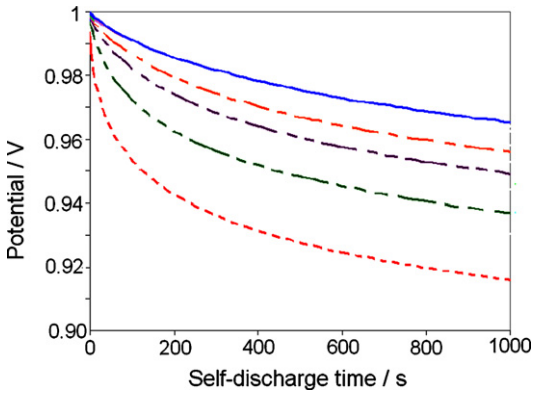

Fig. 2. Self-discharge profile of Spectracarb 2225 (ca. 10 mg) in 1.0 M H_2SO_4 after charging from 0.5 V to 1.0 V at 1 mV s^{-1} and holding at 1.0 V for various times, 0 s ( ), 1 min ( ), 3 min ( ), 5 min ( ) and 10 min ( ).

3. Results and discussion

3.1. Cycling to steady-state

As evidenced by the mirror-image, reversible and almost rectangular cyclic voltammograms seen in Fig. 1, the Spectracarb 2225 is a capacitive material and would be suitable for carbon aqueous ECs. The working electrodes were cycled to steady-state prior to self-discharge measurements. As seen in Fig. 1, this required approximately 300 cycles. During this process quinone groups on the edges of the graphene sheets in the carbon develop, as evidenced by the increasing size of the peaks centered at ca. 0.5 V versus SHE [10–14]. Thus, the working electrodes were cycled to steady-state to ensure that any changes seen in the subsequent self-discharge curves were due to changes in iron-contamination, rather than changes due to quinone group development.

As an important benefit for this work, this week-long cycling procedure also allowed for any minute amount of Fe-contamination due to the carbon to be minimized, since during this cycling procedure any Fe-contaminants will dissolve into the electrolyte and after cycling to steady-state the electrodes are moved to a new electrochemical cell containing clean 1.0 M H_2SO_4 electrolyte. Thus, any Fe-contaminants are left behind in the cell in which the electrode was cycled to steady-state. This ensures that the Fe concentrations used during the contamination studies are known and controllable.

3.2. Effect of adding a holding step on charge redistribution and pore Fe concentration

The carbon used in this work and in carbon-electrode ECs often has a very high electroactive surface area as a result of the highly porous nature of these materials. The high surface areas are required to allow for greater charge storage per geometric area, or per volume. However, because of these small and often torturous pores, the surface at the mouth of the pore charges more quickly during charging than the surfaces deep in the pore [7,8]. That is, an excess of charge on the pore mouth develops versus at the pore base upon completion of charge. When the cell is placed on open-circuit the excess charge at the pore mouth will move down the pore until an even charge distribution is achieved. Since potential is measured at the pore tip in three-electrode measurements, like the self-discharge experiments under study here, this appears as a very rapid loss of potential (see Fig. 2, 0 s holding time). This effect can be mitigated by adding a holding step after electrode charging, allowing more of the surface to reach the desired potential. Longer holding steps lead to much less drastic initial potential drops, as can be seen in Fig. 2. Thus, a 1 h holding time was introduced to all self-discharge measurements to ensure changes in self-discharge profiles during the Fe-contamination studies were actually due to changes in Fe concentration, rather than these charge redistribution effects.

The addition of the holding step may change the Fe concentration in the pores of the electrode, as the Fe will be oxidized/reduced during the holding step. So, various holding steps were examined during the concentrations studies (0 s, 30 min, 1 h and 10 h) to determine if the holding time had any effect on the Fe concentration. It is noted that the Fe-contamination results (charging, holding and Fe-induced trends in the self-discharge profiles) were consistent between these different hold time experiments, suggesting that the holding step does not affect the Fe in the pores. In fact, it is the charging ramp which depletes the reactive Fe in the pore (i.e. when charging to 1.0 V, the Fe^{2+} will all be oxidized to Fe^{3+} when the ramp potential is above 0.77 V, and when charging to 0.0 V, the Fe^{3+} will all be reduced to Fe^{2+}). As seen in Fig. 3a, the current recorded during the holding step is the same for each "bulk" concentration from 0 M to 10^{-3} M, suggesting that, for these bulk electrolyte concentrations, the Fe^{2+} concentration in the pores is 0 M. This full depletion of Fe from the pores is completed during the charging ramp (which is the same for all experiments), and the holding step has no effect on this depletion. This is also what would happen during charging of a "real" EC system. Note, though, that the holding step will affect the amount of charge redistribution due to the pore effect, as the small amount of current which passes during holding (see Fig. 3a inset), is the double-layer charging current as the distributed potential reaches further into the pores.

At concentrations greater than 10^{-3} M, the pore Fe may not be completely depleted during charging, as the current is higher than that for 0 M, indicating that there are some species in the pores to be oxidized. For a 10^{-2} M concentration, this current increase is marginal (see inset Fig. 3a), but is considerable at 10^{-1} M. A similar result is seen for the negative electrode (Fig. 3b), where the Fe^{3+} is essentially depleted at concentrations less than 10^{-2} M, but residual Fe^{3+} remains at higher concentrations.

For 10^{-1} M, the current decays initially and then reaches a steady-state (Fig. 3a), where the Fe^{2+} is likely diffusing into the pores as fast as it is being reacted. This is confirmed by Fig. 3c, where it is shown that this current is constant, even over 10 h of holding. Integration of the current with time indicates that ca. 55 C of charge is passed during this 10 h hold step, which would require ca. 5.5×10^{-4} mol of Fe for reaction (using Faraday's constant and a one electrode oxidation of Fe^{2+} to Fe^{3+}). The amount of Fe in the pores of this carbon can be estimated based on the "bulk" concentration (10^{-1} M), the pore volume for the carbon (1.2 mL g^{-1}) and the pore

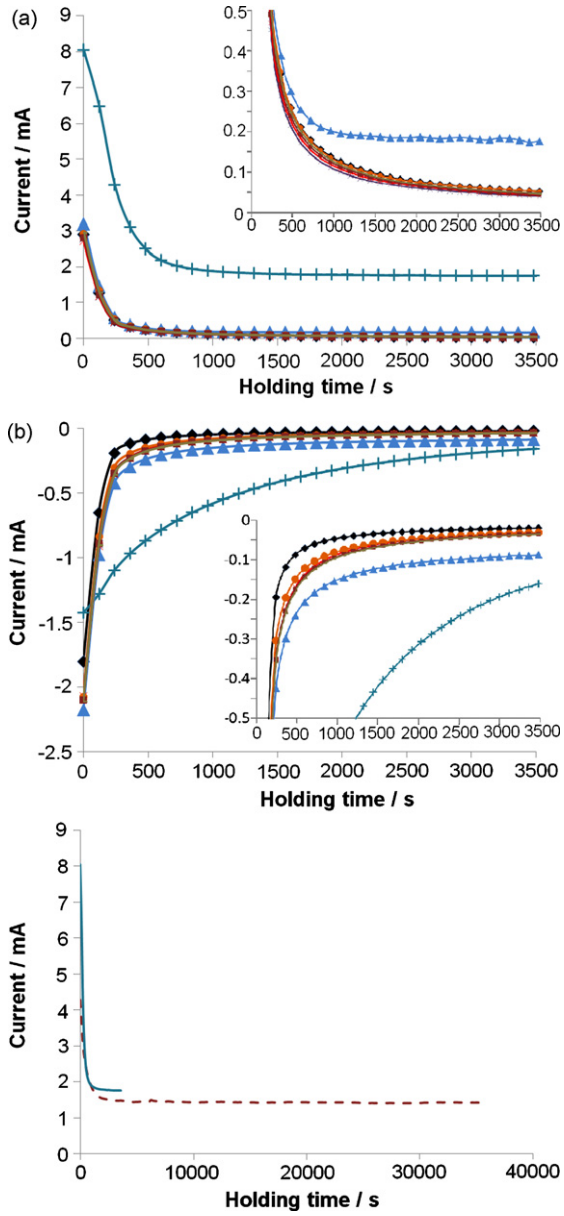

Fig. 3. Current during 1 h holding (a, b) for Spectracarb 2225 carbon cloth in 1.0 M H_2SO_4 contaminated with different concentrations of Fe^{2+} and Fe^{3+} sulfate: 0.0 M (♦), 10^{-8} M ( ), 10^{-6} M ( ), 10^{-5} M ( ), 10^{-4} M ( ), 10^{-3} M (×), 10^{-2} M ( ), 10^{-1} M (+), insets are magnifications at low current. (c) Comparison between current profile for 10^{-1} M electrolytes during hold times of 1 h ( ) and 10 h ( ).

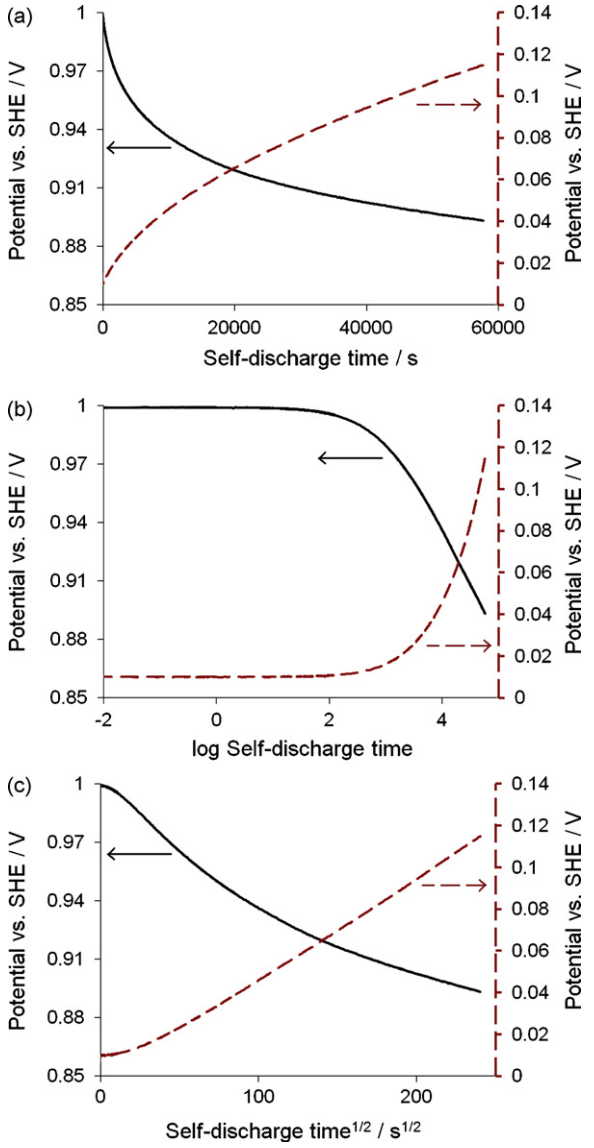

Fig. 4. Self-discharge profile of Spectracarb 2225 in clean (0 M Fe) 1.0 M H_2SO_4 for the electrode charged to 1.0 V (, left axis) and 0.0 V (, right axis), with a 1 h holding time, plotted as voltage as a function of (a) time; (b) log time; and (c) $t^{1/2}$.

mass (10 mg), and it can be shown that there is ca. 1×10^{-6} mol of Fe available in the pores of the carbon, assuming no diffusion. Since the moles of Fe reacted is greater than that available in the pores, Fe must be diffusing into the pores to react. The constant current seen in Fig. 3c, suggests that diffusion is not the rate-limiting step, which would be expected to exhibit a decreasing current with time and the constant current suggests that the system is under convective diffusion-control, caused by the N_2 bubbling. The difference in current between the 1 h and 10 h hold in Fig. 3 is likely due to small differences in N_2 bubbling rate. This steady-state current is reached in both profiles for a 1 and 10 h holding step (Fig. 3c) showing a 1 h hold is sufficient to achieve steady-state, and thus longer hold times do not change the Fe concentrations in the pores.

Considering that there is no difference between the results obtained with the different holding times, that the pore Fe depletion is dependent only on the charging ramp and not the hold times, and that only 1 h of hold time is required to reach the steady-state current exhibited in the 10^{-1} M Fe electrolytes, only the 1 h hold data is presented here.

3.3. Self-discharge profile in the absence of Fe, and comparison with Conway models

The carbon-cloth self-discharge profiles were examined when the electrodes were charged from 0.5 V to either 1.0 or 0.0 V. Fig. 4a shows that even with a 1 h holding time introduced into the charging procedure, there is still significant self-discharge during the 16 h experiments. Part of this self-discharge is likely to be a residual potential drop due to charge redistribution as a 1 h hold may be insufficient to remove all of the pore effects (i.e. 1 h may not be long enough to allow the full surface to charge to the desired potential). The remainder of the self-discharge must be due to at least one, possibly several unidentified self-discharge mechanism(s). These data show that even in an Fe-free system, both electrodes of a

symmetric EC may undergo significant self-discharge. Thus, even with full scrubbing of the Fe from the electrolyte, self-discharge will continue to occur via the other mechanism(s). And, the other mechanism(s) must be identified and minimized to prevent self-discharge in symmetric carbon-electrode, aqueous-electrolyte ECs.

The self-discharge profiles were fit using the Conway models (from Refs. [2] and [3]) in order to learn about their possible self-discharge mechanisms (see Fig. 4b and c). Only the activation-controlled and diffusion-controlled models were examined as the ohmic leakage model is not possible in the three electrode setup used here. When the self-discharge profile of the electrode charged to 1.0 V was plotted as a function of log time (Fig. 4b), a linear plot resulted after an initial plateau (corresponding to the integration constant, θ). This fitting suggests the self-discharge mechanism on the positive electrode is not a diffusion-controlled mechanism (as might be expected if Fe-contamination was the cause), but may be an activation controlled mechanism. The non-linearity of the self-discharge profile when plotted as a function of $t^{1/2}$ (Fig. 4c) confirmed that the mechanism of self-discharge for this electrode, under Fe-free conditions, is not diffusion controlled. This suggests that the unidentified self-discharge mechanism is activation controlled (assuming the Conway models hold for porous electrodes) and, therefore, the reactant species causing self-discharge is either at high concentrations in the cell or is confined to the electrode surface. This may suggest either electrolyte decomposition or carbon surface functionality oxidation/reduction is this, as yet, unidentified self-discharge mechanism.

The opposite situation is seen for the electrode when it is charged down to 0.0 V. Fig. 2b and c, show that the profile is not linear when plotted as a function of log time, but is linear when plotted versus $t^{1/2}$, suggesting that when the electrode is charged to 0.0 V the self-discharge mechanism for the negative electrode relies on the diffusion of a reactive species to the electrode surface (it cannot be Fe, as this is an Fe-free system). Again, this mechanism is unidentified, but is unlikely to be due to electrolyte decomposition or carbon surface functionality oxidation/reduction (as suggested with the electrode charged to 1.0 V). Although N_2 is bubbled through the electrochemical cell during these measurements, the cell is not sealed and a small amount of O_2 may be present in the electrolyte, and it may be that the self-discharge mechanism relies on O_2, but this is still under study.

It should be pointed out, that as expected this data has shown that the electrode has two different self-discharge mechanisms when used as a positive electrode (charged to 1.0 V) or as a negative electrode (charged to 0.0 V) in a symmetric EC. This highlights the necessity of performing three-electrode experiments when determining self-discharge mechanisms, as doing a full-cell experiment may obscure what is truly happening at each electrode. A full understanding of the cause and mechanism of self-discharge at each electrode is required to truly be able to minimize or prevent self-discharge in a cell.

It is surprising to note that the self-discharge profile can be fitted as predicted by the Conway models, as these models were developed for planar electrodes, and the electrodes examined here are highly porous. It is particularly surprising that the diffusion control model fits, as one may expect that in a porous system, one would not only have the semi-infinite diffusion to the electrode surface (as covered by the model), but also diffusion and migration effects down the pores, as well as radial diffusion in the pores. This will be addressed again below, but the agreement between the porous electrode self-discharge profile and the planar self-discharge model may suggest that the electrode is acting as a planar electrode, and it is only the surface of the electrode which participates in the self-discharge, and the pores (particularly deep in the pores) do not contribute to self-discharge.

3.4. Effect of Fe-contamination on self-discharge profiles

3.4.1. Electrodes charged to 1.0 V

The effect of Fe-contamination on self-discharge profiles of the Spectracarb 2225 carbon cloth in 1.0 M H_2SO_4 was examined by incrementally adding $FeSO_4$ and $Fe_2(SO_4)_3$ in equimolar concentrations to the electrochemical cell. The carbon and H_2SO_4 used in this work is essentially Fe-free; however, the carbons and electrolytes used in commercial ECs may have significant Fe-contaminations, leading to the suggestion that Fe may be causing self-discharge. As can be seen in Fig. 5a, there is no significant difference in the self-discharge profile until the electrolyte concentration of Fe reaches 10^{-4} M. This suggests that for systems with Fe concentrations lower than 10^{-4} M, the self-discharge mechanism is not due to an Fe-shuttle on the carbon electrode charged to 1.0 V. This agrees with the predicted mechanism using the Conway models (Section 3.3) which suggested an activation controlled self-discharge mechanism, not diffusion controlled, as might be expected for an Fe-shuttle. This is confirmed for all the low Fe concentrations when the Fe data is plotted as a function of $\log t$ and $t^{1/2}$ (Fig. 5b and c). Thus, for all concentrations up to 10^{-5} M the mechanism is activation controlled and, since all the slopes are identical, it suggests that it is the same mechanism in each case. Again, this mechanism has not yet been identified.

It is unsurprising that at low Fe-concentrations the self-discharge mechanism is not due to an Fe-shuttle for two reasons. The first is that, as shown in Section 3.2, all of the Fe in the pores has been reacted before self-discharge begins, as during charging to 1.0 V all of the Fe^{2+} in the pores is reacted to Fe^{3+}, leaving little to no Fe^{2+} in the pores to be oxidized when the cell is placed on open-circuit to provide the electrons necessary to discharge the positive electrode. This is, in fact, what would happen in a "real" EC system during charging. The second reason is, even if the Fe in the pores was not completely reacted, there is still insufficient Fe in the pores to cause the degree of self-discharge exhibited in Fig. 4. From this figure, it is seen that during the 16 h of self-discharge, the electrode has lost 0.1 V. If it is assumed that a full half of that potential loss is due to charge redistribution, then the potential loss due to the Faradaic reaction is 0.05 V. The capacitance of the electrode near a potential of 1.0 V can be found from Fig. 5 g, and is seen to be ca. 250 F g^{-1}. The charge-density (q, in C g^{-1}) required for a 0.05 V potential loss (V_{loss}) at this capacitance (C) can be calculated from

$$q = \frac{C}{V_{loss}} \tag{4}$$

resulting in a required charge-density of 12.5 C g^{-1}. The mass of the electrode is ca. 10 mg, meaning 0.125 C of charge (Q) is needed to cause this self-discharge. Assuming no diffusion down the pores, the Fe concentration required for this degree of self-discharge can be calculated from

$$[\mathrm{Fe}] = \frac{Q}{FVm} \tag{5}$$

where F is Faraday's constant, V is the pore volume per gram of material (1.2 mL g^{-1} for Spectracarb 2225) and m is the mass of the carbon. Using this calculation, ca. 0.1 mol L^{-1} of Fe is required in the pores for this degree of self-discharge. Obviously, there is insufficient Fe in the pores to cause this self-discharge at these low Fe concentrations.

Fig. 5b shows that at concentrations above 10^{-4} M, the self-discharge profile deviates away from linearity on the $\log t$ scale, suggesting it is no longer activation controlled. When the data is plotted as a function of $t^{1/2}$ (Fig. 5c) the linearity of the plot at 10^{-4} M indicates a diffusion controlled mechanism. Additionally, Fig. 5d shows at concentrations above 10^{-4} M, an increase in Fe

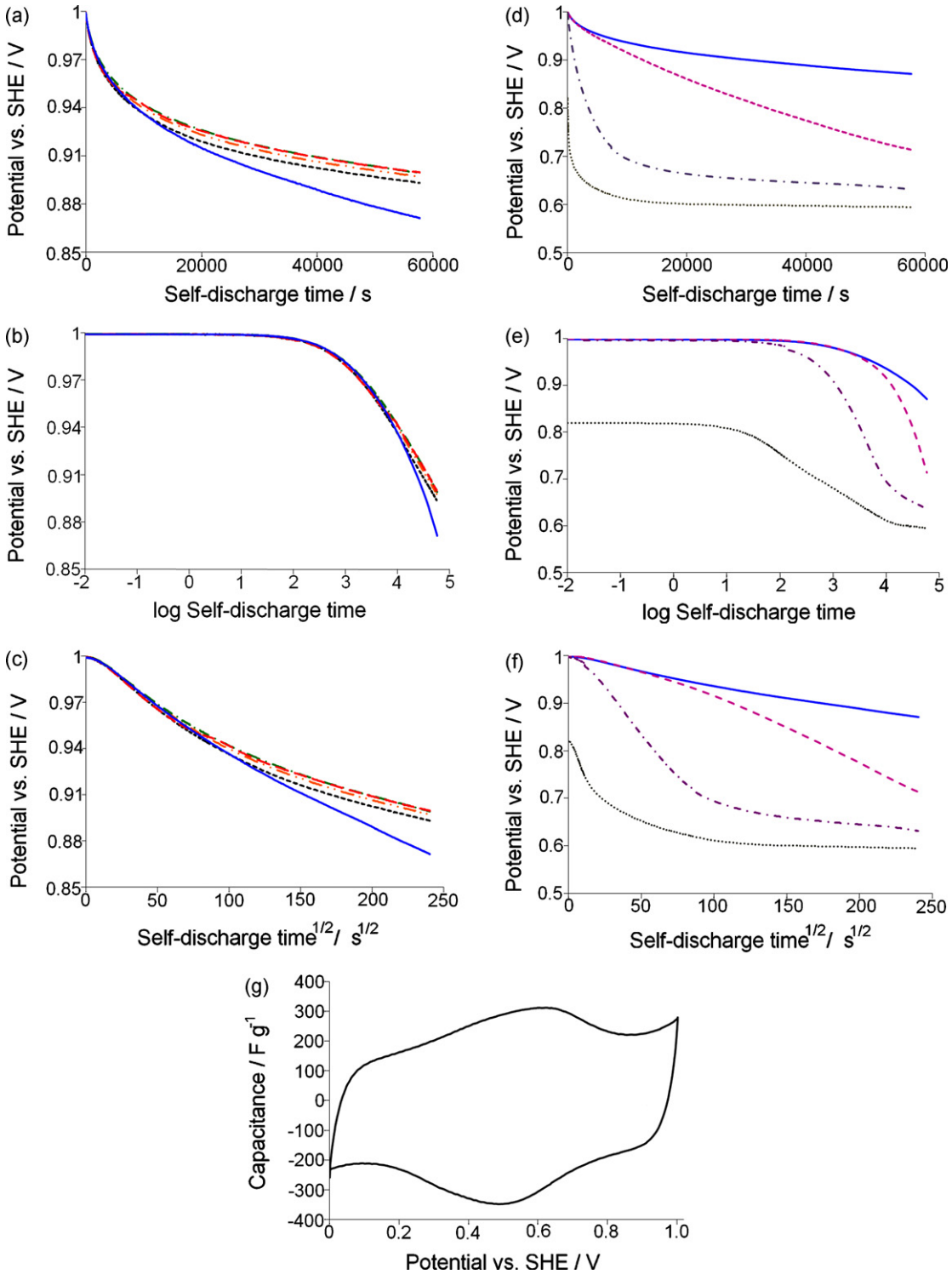

Fig. 5. Self-discharge profiles (a–f) and differential capacitance profile (g) for Spectracarb 2225 carbon cloth charged to 1.0 V in 1.0 M H_2SO_4 contaminated with various concentrations of Fe^{2+}/Fe^{3+} sulfate: (a–c) 0 M (——), 10^{-8} M (—●●—), 10^{-6} M (—●—), 10^{-5} M (– –), 10^{-4} M (——), and (d–f) 10^{-4} M (——), 10^{-3} M (– –), 10^{-2} M (—●—), 10^{-1} M (●●●).

concentrations leads to an increase in self-discharge. This confirms that we have changed the mechanism of self-discharge and at concentrations greater than 10^{-4} M the Fe in the cell will act as a shuttle to discharge the cell.

As expected, the self-discharge profile for Fe concentrations of 10^{-4}, 10^{-3} and 10^{-2} M are all diffusion controlled (Fig. 5e and f), exhibiting linear potential versus $t^{1/2}$ profiles, at least in part. For the 10^{-2} M concentration, the profile deviates from a linear $t^{1/2}$ plot at a potential of ca. 0.7 V. It is suggested that at this potential the electrode is nearing its open circuit potential for the system and therefore the rate of self-discharge is diminished. For even higher concentrations, the self-discharge profile no longer can be fit with the Conway models. Interestingly, this concentration corresponds to that calculated above to be the point at which the Fe in the

Table 1
Time and potential of deviation of self-discharge data collected at 10^{-4} M Fe vs. 0 M Fe self-discharge for different holding times.

Holding time (min)	Time at deviation (h)	Potential at deviation (V)
0	4 ± 2	0.88 ± 0.01
30	3 ± 1	0.92 ± 0.01
60	7 ± 3	0.91 ± 0.01

The errors show one standard deviation.

pores may be sufficient to discharge the electrode without requiring diffusion, although diffusion, of course, still occurs. Thus, it is suggested that the profile of the 10^{-2} M Fe concentration is likely a combination of Fe-induced self-discharge which is activation controlled and diffusion controlled.

It is also interesting to note that for 10^{-4} M and 10^{-3} M, the self-discharge mechanism is not diffusion controlled at high potentials. In fact, the profile for the 10^{-4} M shows that at potentials above ca. 0.9 V, the self-discharge mechanism is the same as that previously seen at lower Fe concentrations. This suggests either charge redistribution is still the main contributor to self-discharge in this time domain (despite the 1 h holding step), some other activation controlled self-discharge mechanism is responsible for self-discharge above this potential or the Fe concentration in the pores is sufficient to not be diffusion limited. There are two arguments against the latter possibility. First, the agreement between the data for 10^{-4} M and that for lower concentrations suggests Fe in not the main self-discharge mechanism here, as it was shown earlier that at the low concentrations Fe does not contribute to the self-discharge. Secondly, based on the calculation above, and the results in Section 3.2 which showed complete depletion of the Fe in the pores during charging, it is unlikely that the Fe concentration in the pores is sufficiently high enough to cause this degree of self-discharge. Indeed, it can be seen in Fig. 5 that at higher concentrations (e.g. 10^{-3} M in Fig. 5f), this region of the self-discharge profile changes, suggesting that 10^{-4} M is not a high enough concentration to account for this activation control region. Thus, the two other possibilities are more likely.

In order to examine whether the pore effect (leading to charge redistribution) was the main self-discharge process at these high potentials and short self-discharge times, different hold times were introduced into the electrode-charging regime. Presumably, longer holding times would result in a more even potential being reached in the pores, leading to less charge redistribution and a shorter initial period before Fe-induced self-discharge takes over. Conversely, if the self-discharge at short self-discharge times (high potentials) is due to a different Faradaic reaction (the oxidation of an unknown species), then the holding time would be irrelevant and the *potential* where Fe-induced self-discharge takes over would be constant. Thus, the time and potential required for the self-discharge profile at 10^{-4} M Fe to deviate more than 10 mV from the self-discharge profile at 0 M was determined. The data in Table 1 show the results for a hold time of 0, 30 and 60 min. As can be seen from this table, there is no trend in the self-discharge time required for deviation to occur, with times for individual electrodes varying significantly. However, the potential of deviation is reasonably constant, with deviation occurring at ca. 0.90 ± 0.02 V. These results suggest that at high potentials self-discharge is not dominated by charge redistribution, but rather is due to the oxidation of an unknown species. The unidentified redox reaction must be an oxidation, as it is the loss of electrons of the Faradaic process which discharges the positive electrode. There are two possibilities as to why this new oxidation has become the main mechanism of self-discharge at potentials above 0.9 V. First, it may be kinetically faster than $Fe^{2+} \rightarrow Fe^{3+}$ oxidation at these potentials. Second, the concentration of Fe at the surface of the electrodes has fallen to zero (limiting current conditions) and the kinetics of the unidentified reaction is faster than the diffusion of iron. This is supported by the fact that at higher concentrations of Fe, which would result in faster diffusion (due to the steeper concentration gradient), the Fe-induced self-discharge becomes the dominant self-discharge mechanism at higher potentials (Fig. 5), hence at these high concentrations diffusion is faster than the kinetics of the unidentified reaction. This unidentified reaction is under study in the authors' laboratory. It may be that the carbon electrode is undergoing carbon oxidation to CO or CO_2 (thermodynamically favoured above ca. 0.9 V), similar to that seen in fuel cells [15–17]. However, it should be noted that there is no Pt catalyst in ECs as with fuel cells, thus one might expect carbon oxidation to be kinetically slower in ECs. Nevertheless, it is thermodynamically possible.

Conveniently, the addition of a hold time also tests the argument that Fe is at sufficiently high concentrations to not be diffusion controlled, as longer hold times will result in more thorough conversion of Fe^{2+} to Fe^{3+} and less Fe^{2+} remaining in the pores. Thus, at longer hold times diffusion control should dominate at earlier self-discharge times since the Fe^{2+} would be used up in the pores and would need to diffuse in from the bulk electrolyte. Again, this is not supported by the data in Table 1, confirming that Fe is not the main self-discharge mechanism at these potentials.

Interestingly, for all of the different hold times examined, the Fe concentration at which the self-discharge profile began to be dependent on the Fe shuttle was 10^{-4} M. This was surprising as long hold times may be expected to deplete the Fe inside the pores to a greater extent than short hold times, and thus with long hold times there would be insufficient Fe to allow for Fe-induced self-discharge; whereas short hold times may leave sufficient Fe to induce self-discharge. Therefore, for longer hold times, it would be expected that a higher Fe concentration would be required before Fe-induced self-discharge was in evidence. The fact that all systems begin to demonstrate Fe-induced self-discharge at 10^{-4} M suggests it is *not* the pore Fe concentration which is the limiting factor, but rather the bulk concentration. This implies the self-discharge does not occur in the pores but is, rather, primarily occurring on the electrode surface (at the pore mouth). This is easily rationalized in that the Fe^{2+} in the pores has been depleted during charging (see Section 3.2), and thus more Fe^{2+} must diffuse in from the bulk to allow self-discharge to occur. As the Fe^{2+} diffuses in, it will react as soon as it encounters the electrode, which is likely to be on the surface of the electrode, or, at most, only a very short distance down the pores. Thus, this result gives the first real indication about where on the electrode surface the self-discharge processes are actually occurring. As well, this likely is the explanation for the fact that the Conway diffusion model is able to fit the self-discharge profiles for porous electrodes, even though they are derived for semi-infinite diffusion to a planar electrode. Since the pores are essentially depleted of Fe and therefore cannot participate in the self-discharge process, the pores essentially become "invisible" to self-discharge and the electrode appears simply as a nearly planar surface, such as would be appropriate for the Conway model.

Based on the above discussion, it should theoretically be possible to increase the Fe concentration such that the Fe content in the pores is sufficient to discharge the electrode without reliance on diffusion (based on the above calculations, this concentration is likely at or above 0.1 mol L^{-1}), and this may be the cause of the fact that the Conway models cannot fit the self-discharge profile at 0.1 M Fe concentrations. In practice, however, at concentrations above 0.1 M, the oxidation of Fe^{2+} proceeds to such an extent during charging that the desired potential of 1.0 V cannot be reached (see the initial potential of the 10^{-1} M trace in Fig. 5f), and the electrode cannot be fully charged.

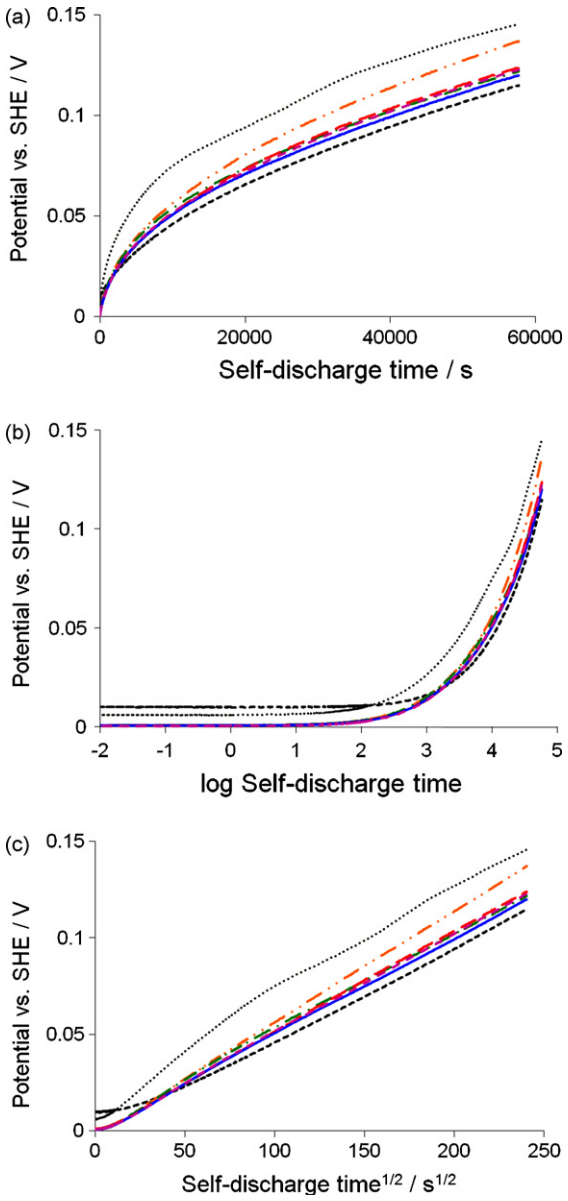

Fig. 6. Self-discharge profiles for Spectracarb 2225 carbon cloth charged to 0.0 V in 1.0 M H_2SO_4 contaminated with various concentrations of Fe^{2+}/Fe^{3+} sulfate: 0 M ( ), 10^{-8} M ( ), 10^{-6} M ( ), 10^{-5} M ( ), 10^{-4} M ( ), 10^{-3} M ( ), 10^{-1} M ( ).

3.4.2. *Electrodes charged to 0.0 V*

The Fe-induced self-discharge of the negative carbon electrode in an asymmetric Pb/C EC has been studied at high Fe concentrations by Kazaryan et al. [5]. The effect of Fe concentration on the self-discharge of the negative carbon electrode in a three-electrode configuration at low Fe concentrations was examined here. As discussed in Section 3.2, the self-discharge profile for the carbon electrode when it is charged negatively fits with the Conway diffusion model when a Fe-free electrolyte is used. As shown in Fig. 6, within the error of the experiment, the Fe concentration does not affect the self-discharge profile up to concentrations of 10^{-3} M, although with all of the electrodes examined, the self-discharge profile of the electrolyte containing 10^{-1} M Fe shows a more rapid self-discharge, suggesting that at this high concentration, the Fe is participating in the self-discharge. This is unlike the results on the positive electrode, where Fe-induced self-discharge begins at 10^{-4} M. Thus, the negative electrode is much less susceptible to Fe-induced self-discharge and can withstand greater Fe-contamination concentrations without enhanced self-discharge. This is a benefit for asymmetric ECs where carbon is often used for the negative electrode.

Nevertheless, this negative electrode does show self-discharge and the mechanism of this self-discharge is unknown. The shape of the curves in Fig. 5c (for concentrations up to 10^{-3} M) show the mechanism is diffusion controlled, meaning this reaction must rely on a low concentration solution species. Given the linear region of Fig. 5c begins almost immediately, and there is no change in the slope over the 16 h self-discharge, this suggests only one mechanism is responsible for the discharge of the negative electrode. This mechanism is under study in the authors' laboratory. Since N_2 is bubbled into the electrochemical cell during the measurements but the cell is not sealed, it may be some small O_2 content in the electrolyte which is undergoing reduction to H_2O or H_2O_2. As Fig. 5 shows, there is much less consistency between the self-discharge profiles for the electrodes when charged to 0.0 V versus that seen when charged to 1.0 V, and it may be small variations in the electrolyte O_2 content which is responsible for this variation in self-discharge rates. Nevertheless, the data consistently shows a lack of relationship between Fe concentration and self-discharge rate until 10^{-3} M, above which an increase in Fe concentration leads to an increase in self-discharge rate.

4. Conclusions

It was shown that for a symmetric carbon-based, aqueous-electrolyte EC, the self-discharge mechanism on the positive and negative electrodes are different and should be studied with a three-electrode (half cell) setup. In an H_2SO_4 electrolyte which is free of Fe-contamination the positive electrode has a self-discharge profile which is predicted to be activation controlled as per the Conway models. Conversely, the self-discharge mechanism for the negative electrode in the same situation is predicted to be diffusion controlled.

No Fe-induced self-discharge is seen at concentrations up to 10^{-5} and 10^{-3} M for the positive and negative electrodes respectively. At intermediate Fe-concentrations, the Fe-shuttle mechanism does become the major self-discharge mechanism, and it is diffusion controlled. Importantly, it was shown the Fe-induced self-discharge occurs primarily on the exterior surface of the porous electrodes and the pores do not take part in the Fe-induced self-discharge mechanism. This is due to the depletion of the Fe in the pores during charging. This can be used to explain the fact that the Conway diffusion control self-discharge model, which was derived for semi-infinite diffusion to a planar electrode is able to fit the self-discharge profile of a porous electrode.

At high Fe concentrations (e.g. 10^{-1} M) Fe-induced self-discharge is still the main self-discharge mechanism; however, at these concentrations, the system is no longer diffusion controlled and the rate-limited step is the reaction of Fe on the carbon surface.

Acknowledgements

The authors would like to gratefully acknowledge the Natural Sciences and Engineering Research Council of Canada (NSERC) for support for this research, as well as Trisha Huber and Scott McClelland at Defence R&D Canada, Atlantic Dockyard Lab Pacific, for ICP-MS measurements of Fe-contamination in Spectracarb 2225. Finally, Axion Power International, Ltd. for supplying the current collectors used in this work.

References

[1] B.E. Conway, Electrochemical Supercapacitors: Scientific Fundamentals and Technological Applications, Kluwer-Plenum Publ. Co, New York, 1999.
[2] B.E. Conway, W.G. Pell, T. Liu, J. Power Sources 65 (1997) 53–59.
[3] J. Niu, W.G. Pell, B.E. Conway, J. Power Sources 156 (2006) 725–740.
[4] B. Pillay, J. Newman, J. Electrochem. Soc. 143 (1996) 1806–1814.
[5] S.A. Kazaryan, G.G. Kharisov, S.V. Litvinenko, V.I. Kogan, J. Electrochem. Soc. 154 (2007) A751–A759.
[6] S.A. Kazaryan, S.V. Litvinenko, G.G. Kharisov, J. Electrochem. Soc. 155 (2008) A464–A473.
[7] R. de Levie, Electrochim. Acta 8 (1963) 75180.
[8] R. de Levie, Electrochim. Acta 9 (1964) 1231–1245.
[9] D.R. Lide (Ed.), CRC Handbook of Chemistry and Physics, 88th ed., CRC Press, 2007–2008.
[10] K. Okajima, K. Ohta, M. Sudoh, Electrochim. Acta 50 (2005) 2227–2231.
[11] J.V. Hallum, H.V. Drushel, J. Phys. Chem. 62 (1958) 110–117.
[12] H.V. Drushel, J.V. Hallum, J. Phys. Chem. 62 (1958) 1502–1505.
[13] V.A. Garten, D.E. Weiss, Aust. J. Chem. 8 (1955) 68–95.
[14] H.P. Boehm, Adv. Catal. 16 (1966) 179–274.
[15] S.I. Pyun, Y.G. Ruy, S.H. Choi, Carbon 32 (1994) 161–164.
[16] H. Binder, A. Koehling, K. Richter, G. Sandstede, Electrochim. Acta 9 (1964) 255–274.
[17] J. Willsau, J. Heitbaum, J. Eletroanal. Chem. 161 (1984) 93–101.